Safety Assessment of AIMDs under MRI Exposure: Tier3 vs. Tier4 Evaluation of Local RF-induced Heating

Eugenia Cabot*, Earl Zastrow*,†, and Niels Kuster*,†
*IT'IS Foundation, Zurich, Switzerland, Email: cabot@itis.ethz.ch
†Department of Information Technology and Electrical Engineering (D-ITET), ETH-Zurich, Zurich, Switzerland

***Abstract*—Patients with active implantable medical devices (AIMDs) are generally excluded from magnetic resonance (MR) diagnostics because interference of the AIMD with MR-induced radiofrequency (RF) fields can lead to hazardous localized heating in the surrounding tissues. In this work, we report the safety assessment of a generic device performed according to tier 3 and 4 guidelines in Technical Specification 10974. For tier 3, local tissue heating was obtained by applying RF fields, obtained numerically *in vivo* in human models exposed to MRI coils, to a transfer function of the device. For tier 4, a validated model of the generic device was implanted in anatomical human models exposed to the RF of MRI coils, and full-wave computational electromagnetic simulations were performed. A comparison of the two methods is made.**

Keywords—MRI; Medical Devices; Safety.

I. INTRODUCTION

Magnetic resonance imaging (MRI) is a medical diagnostic technique that yields high-quality images of the inner tissues of the human body. In particular, MRI allows visualization of soft tissues with a higher contrast than afforded by other imaging techniques, such as computed tomography (CT) and, unlike the latter, without ionizing radiation.

In general, patients who have been fitted with an active implantable medical device (AIMD), such as a pacemaker or a deep brain stimulator, are not eligible for MRI diagnostic procedures for reasons of safety concerning the interaction of the radio frequency (RF) electromagnetic fields (EMFs) produced by the MRI scanner and the conductive parts of the AIMD. This coupling mechanism generates high local energy deposition in the tissue surrounding the conductive terminations, e.g., electrodes, and the heating consequently generated may cause irreversible damage to the tissue. Several theoretical ([1], [2]) and experimental studies ([3],[4]) substantiate the large parameter range of the problem and indicate that temperature increases in the tissue can easily reach several tens of degrees. As a consequence, patients with AIMDs are excluded from the benefits of MRI diagnostics, unless the AIMD qualifies for 'MRI conditional' labeling by regulatory bodies.

MRI-safe implants are technically feasible, and most manufacturers are striving towards their development. To be able to reliably assess realistic worst-case temperature increases of such implants during MRI examinations, regulators and implant manufacturers need appropriate methodologies, instrumentation, and procedures.

These safety issues have been recognized by a joint working group of the ISO and the IEC, who have developed the first edition of a technical specification (TS) for the demonstration of the safety of AIMDs for patients undergoing MRI diagnostics at 1.5T 0. TS10974 addresses several MRI-related hazards of AIMDs, among which is the risk of RF-induced tissue heating, and a four-tier approach has been developed to evaluate this risk. The lower tiers yield overestimations of the temperature increase and, therefore, a high safety margin. The higher tiers reduce the overestimation, but require accurate quantification of the incident fields or modeling of the AIMD placed in a sufficiently large set of anatomical body models exposed to the RF fields of MRI scanners. The second edition of the TS, currently under development, includes improvements of the procedures to follow for safety assessment.

In this work, the safety in terms of MRI-heating of a generic AIMD was evaluated according to tiers 3 and 4 in TS 10974. The two methods are compared by applying them for the safety assessment of a generic AIMD.

II. METHODS

A. Description of the Generic AIMD

The selection of a canonical structure as the generic AIMD simplifies the numerical evaluations. The generic AIMD consists of an insulated 800 mm long, 0.75 mm radius stainless steel wire, with an insulation radius of 1.25 mm. The wire is capped at one end and has a 10 mm long bare segment at the other end.

The MR-safety assessment with respect to RF-heating was performed for this generic AIMD according to the procedures specified in TS 10974 for tiers 3 and 4.

B. Description of the Safety Assessment Following Tier 3

With the tier 3 assessment, we evaluate the *in vivo* power deposition around the implant electrode by applying the incident magnitude and phase of the EMF distributions to a validated electromagnetic (EM) model of the AIMD. The tier 3 assessment consists of 3 distinct tasks: assessment of the *in vivo* fields incident to the patients in an MRI environment, development of a validated EM model of the AIMD, and

assessment of the *in vivo* power deposition of the AIMD from electric field (E-field) coupling.

The *in vivo* incident fields are obtained from EM modeling of the RF-human interactions under exposure from the transmit coil of an MRI scanner. Numerical full-wave simulations were performed to assess the EM exposure of human anatomical models to the RF fields of an MRI scanner. For that, a numerical model of the RF coil in the MRI scanner (1.5 T) was built and validated [5]. The coil was loaded with a range of human phantoms covering the patient population in all clinically relevant scan positions [6] (see Fig. 1 for an example). Simulations were performed with SEMCAD X, a platform developed by SPEAG, Zurich, based on the finite-difference time-domain method (FDTD) [7].

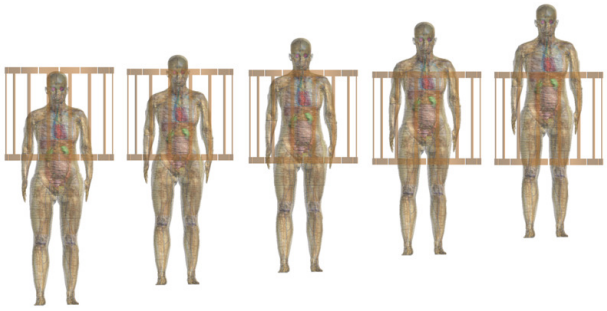

Fig. 1. Ella model from the Virtual Population at a selection of landmarks in the birdcage coil.

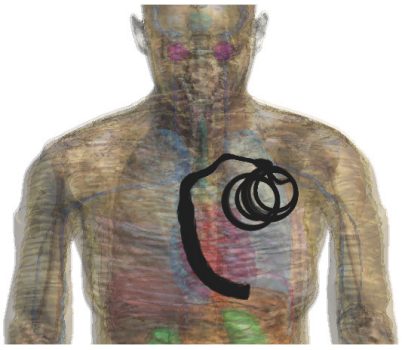

Fig. 2. Sample trajectories for cardiac routing.

The E-fields induced in the body are responsible for the coupling mechanism produced in the conductive parts of the implants and, therefore, need to be studied at the location of the implant. For that purpose, sets of realistic clinical trajectories that represent the possible positions of the devices in the human body were created for the study of the *in vivo* E-fields at these locations. The E-fields tangential to these trajectories represent the E-fields incident to the AIMD. The assessment of the *in vivo* fields needs to be performed for the patient population and all clinically relevant implant positions. A group of trajectories that mimic the routing of cardiac implants is shown for the Ella model in Fig. 2. The average and 95th percentiles of the magnitude of the E-fields tangential to the trajectories are plotted as a function of trajectory length in Fig. 3(a), and the phases of the E-fields tangential to the trajectories are plotted in Fig. 3(b).

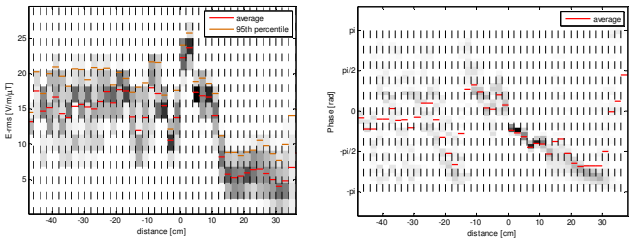

(a) (b)

Fig. 3. Tangential E-fields to the 800 mm cardio trajectories for the *in vivo* field assessment: (a) Magnitude in V/m/µT, (b) Phase in radians.

The equivalent EM model of the generic AIMD was developed numerically. This model characterizes the local RF-induced heating in the AIMD. The characterization is based on the method introduced in [2], where a transfer function to relate the local induced electric field around an electrode of an AIMD to an excitation along the length of the AIMD is defined. The magnitude and phase of the transfer function is shown in Fig. 4.

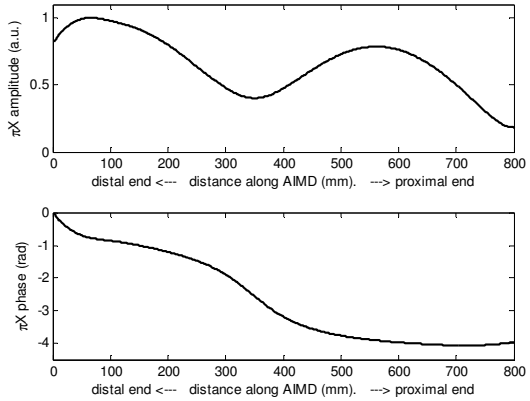

Fig. 4. Magnitude and phase of the transfer function of the generic AIMD.

The distribution of *in vivo* local power deposition is computed at the conductive electrode by exciting the validated model in Fig. 4 with the extracted *in vivo* incident fields in Fig. 3. The *in vivo* local power deposition is computed according to the following expression

$$P = \mathrm{A}\left|\int_0^L h(l)E\tan(l)dl\right|^2$$

where A is a constant, P is the local power deposition of the AIMD at the electrode, $h(l)$ is the validated model of Fig. 4, and $E\tan(l)$ is the *in vivo* E-field tangential to the trajectories determined as previously explained. The resulting distribution is a prediction of the *in vivo* power deposition accurate within the combined uncertainty budget of the AIMD model and the *in vivo* incident E-fields.

C. Description of the Safety Assessment Following Tier 4

For tier 4, full-wave computational EM simulations were performed with the implant model placed in realistic clinical routings inside anatomical phantoms. The implanted human models were then exposed to the RF fields of an MRI body coil.

Several simulations have been performed with the adult female Ella model implanted with the generic AIMD along different clinical routings and exposed to the fields of the body coil. In Fig. 5, a sample of the generic AIMD implanted in the Ella model of the Virtual Population is shown. The plot shows how the generic AIMD is implanted along one relevant clinical trajectory, as well as the SAR enhancement at the tip of the lead due to RF heating.The lead goes from the pectoral region to the insertion point in the vein, follows the path in the vein up to the heart chamber, and ends with the electrode in the heart apex region.

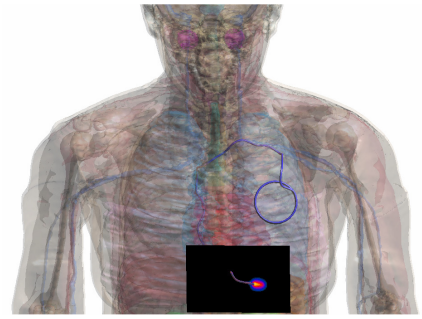

Fig. 5. Sample of the generic AIMD along a clinical cardiac routing in the Ella model of the Virtual Population. The enhancement of the SAR at the electrode of the generic AIMD is also shown.

Full-wave simulations with the implanted AIMD along different clinical trajectories have been performed. Fig. 6 shows part of the torso of the Ella model with the implanted AIMD in a selected subset of configurations, as well as the nomenclature used for identification of each of the routings along trajectories 1 – 6 (T1 – T6).

The peak SAR averaged over 10 mg (SAR10mg) has been computed for each of the configurations. However, for a complete tier 4 evaluation, a comprehensive set of simulations that cover all clinically relevant trajectories should be performed, and the power deposition should be assessed with the corresponding uncertainty budget.

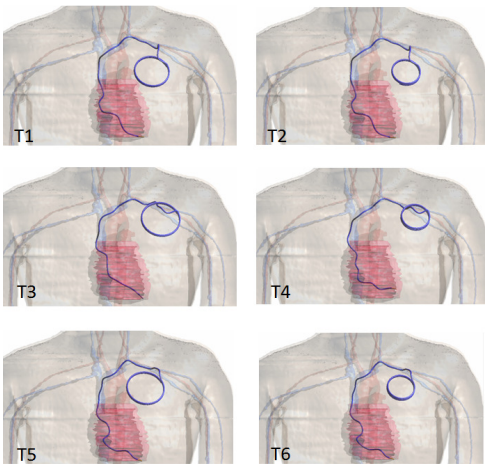

Fig. 6. Subset of the full-wave simulations performed for the safety assessment of the generic AIMD according to the procedure in tier 4. The images show part of the torso of the Ella model with the generic AIMD implanted in different configurations.

III. RESULTS

The results of the safety assessment of the AIMD performed by the two methods presented in section II are summarized in Fig. 7 and TABLE I. The SAR10mg values are normalized to the normal operating mode, which imposes a limit of 2 W/kg for the whole body SAR [8].

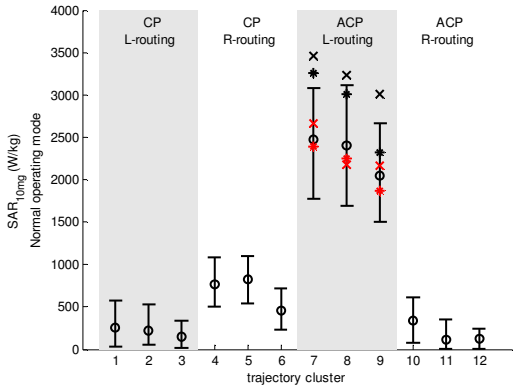

Fig. 7. Summary of the SAR10mg assessment at the tip of the generic implant for the two methods. The error bars indicate the minimum, maximum, and average SAR10mg for a given group of incident field conditions: circular polarization (CP) vs. anti-circular polarization (ACP), and left (L) or right (R) routing. Each of the 3 error bars per group corresponds to a trajectory cluster ending in a certain pectoral region. The symbols '*' and 'x' stand for T1, T3, and T5, and T2, T4, and T6, respectively, and are red for tier 3 and black for tier 4. The SAR10mg values are also summarized in TABLE I.

TABLE I. SAR10MG AT THE ELECTRODE OBTAINED WITH THE TIER 3 AND TIER 4 ANALYSES FOR THE SELECTED SUBSET OF IMPLANT ROUTINGS SHOWN IN FIG. 6. THE DEVIATION OF THE SAR10MG IN DB FOR THE TWO METHODS IS ALSO LISTED. THE SAR10MG VALUES ARE GIVEN FOR THE NORMAL OPERATION MODE LIMIT

	Tier 3: SAR10mg [KW/kg]	**Tier 4: SAR10mg [KW/kg]**	**Deviation [dB]**
T1	2.39	3.26	1.35
T2	2.67	3.46	1.13
T3	2.25	3.01	1.26
T4	2.18	3.24	1.72
T5	1.87	2.32	0.94
T6	2.17	3.01	1.42

A graphical representation of the statistical analysis of the tier 3 assessment is shown in Fig. 7. The error bars indicate the minimum, maximum, and average SAR10mg at the AIMD electrode for a group of incident field conditions: circular polarization (CP) vs. anti-circular polarization (ACP), and left (L) or right (R) routing, depending on the side of the body where the implant is located. The highest power deposition predictions at the electrode of the implant occur for ACP and L-routing. The values of the SAR10mg resulting from the full-wave computational simulations performed in the frame of the tier 4 analysis are shown in Fig. 7 as black '*' and 'x' symbols; the tier 3 values for the same trajectories are shown in the plot as red '*' and 'x' symbols. The values of the SAR10mg obtained by the two methods are summarized in TABLE I. The deviation of the SAR10mg at the electrode of the generic AIMD for the two methods in the subset of selected trajectories ranges from 0.94 dB to 1.72 dB.

IV. CONCLUSIONS

In this work, the safety assessments of a generic AIMD were performed according to tier 3 and 4 guidelines in TS 10974. For tier 3, the local tissue heating was obtained by applying the *in vivo* fields obtained numerically in human models exposed to RF fields from MRI coils, to a transfer function of the AIMD. For tier 4, a validated model of the generic device was implanted in anatomical human models exposed to the RF of MRI coils. The preliminary evaluation and comparison of the two methods yields a deviation range of 0.94 – 1.72 dB in the SAR10mg deposited at the electrode of the generic AIMD. For a complete tier 4 analysis, the simulation sample pool must be considerably increased.

REFERENCES

[1] W. Nitz, A. Oppelt, W. Renz, C. Manke, M. Lenhart, J. Link, "On the heating of linear conductive structures as guide wires and catheters in interventional MRI", *J. Mag. Res. Imag.*, vol. 13(1), 105–114, January 2001.

[2] S. Park, R. Kamondetdacha, J. Nyenhuis, "Calculation of MRI-induced heating of an implanted medical lead wire with an electric field transfer function", *J. Magn. Reson. Imag.*, vol. 26, pp. 1278–1285, November 2007.

[3] R. Luechinger, V. Zeijlemaker, E. Pedersen, P. Mortensen, E. Falk, F. Duru, R. Candinas, P. Boesiger , "*In vivo* heating of pacemaker leads during magnetic resonance imaging", *Eur. Heart J.*, vol. 26(4), 376–383, February 2005.

[4] P. Nordbeck, I. Weiss, P. Ehses, O. Ritter, M. Warmuth, F. Fidler, V. Herold, P. Jakob, M. Ladd, H. Quick, et al., "Measuring RF-induced currents inside implants: Impact of device configuration on MRI safety of cardiac pacemaker leads", *Magn. Reson. Med.*, vol. 61(3), pp. 570–578, 2009.
ISO TS 10974, "Assessment of the safety of magnetic resonance imaging for patients with an active implantable medical device", 1st Edition. Geneva, Switzerland, 2012.

[5] E. Cabot et al., "Evaluation of the RF Heating of a Generic Deep Brain Stimulator Exposed in 1.5T MR Scanners", *Bioelectromagnetics,* vol. 34 (2), pp.104–113, February 2013.

[6] A. Christ et al., "The virtual family: Development of surface-based anatomical models of two adults and two children for dosimetric simulations", *Phys. Med. Biol.*, vol. 55, pp. N23–N38, 2010.

[7] A. Taflove, S.C. Hagness, Computational electromagnetics: The finite-difference time-domain method, 2nd ed. Boston, USA, London, United Kingdom: Artech House. 2000.

[8] IEC60601-2-33, "Particular requirements for the basic safety and essential performance of magnetic resonance equipment for medical diagnosis", 2010.